Supplementary material

Natural deep eutectic solvent-based aqueous biphasic system coupled with MoS_2 photocatalytic reduction for green recovery of gold from thiosulfate solution

Guiping Zhu,[a] Junhui Yu,[a] Ru Zhang,[a] Ding Chen,[a] Xiaoyu Ma,[a] Lingling Zhao,[a] Qilan Huang,[a] Xiangjun Yang,*[a] Shixiong Wang,*[a]

[a] Research Center of Lake Restoration Technology Engineering for Universities of Yunnan Province, School of Chemical Science and Technology, Yunnan University, Kunming, China.

*Corresponding Author at: School of Chemical Science and Technology, Yunnan University, No. 2, CuiHu North Road, Kunming, Yunnan Province 650091, China.

E-mail: yxjun@ynu.edu.cn (X. Yang); wangshixiong@ynu.edu.cn (S. Wang)

Number of pages in Supporting Information: 29

Number of tables in Supporting Information: 7

Number of figures in Supporting information: 9

Number of texts in Supporting information: 7

Contents

2. Material and methods

2.1. Chemicals

Table S1. Chemicals

Reagent	Content	Manufacturer (Company)
Betaine hydrochloride	99.0%	Adamas Chemical reagent
Choline chloride	99.0%	Adamas Chemical reagent
Acetic acid glacial	99.0%	Adamas Chemical reagent
Propionic acid	99.0%	Adamas Chemical reagent
Malonic acid	99.0%	Adamas Chemical reagent
Butyric acid	99.0%	Adamas Chemical reagent
Ethylene glycol	99.0%	Adamas Chemical reagent
D-(+)-glucose	99.0%	Adamas Chemical reagent
D-(-)-fructose	99.0%	Adamas Chemical reagent
Potassium phosphate tribasic	99.0%	Adamas Chemical reagent
Sodium thiosulfate	99.0%	Adamas Chemical reagent
Thiourea	99.0%	Adamas Chemical reagent
Molybdenum (IV) sulfide	99.0%	Adamas Chemical reagent
Itaconic acid	99.0%	Adamas Chemical reagent
DL-Malic acid	99.8%	Adamas Chemical reagent
Sorbic acid	99.8%	Adamas Chemical reagent
2-Propanol	99.8%	Adamas Chemical reagent
1,3-Propanediol	99.8%	Adamas Chemical reagent
Cupric chloride anhydrous	99.8%	Adamas Chemical reagent
Dimethyl sulfoxide-d6	99.8%	Adamas Chemical reagent
Cobalt chloride	99.8%+	Adamas Chemical reagent
Methyl alcohol	99.9%	Adamas Chemical reagent
1-Butanol	99.9%	Adamas Chemical reagent
Xylitol	99.9%+	Adamas Chemical reagent
Ammonium molybdate(VI) Tetrahydrate	99.9%+	Adamas Chemical reagent
Lithium hydroxide	99.9%+	Adamas Chemical reagent
Gold	99.99%	Adamas Chemical reagent
Lactic acid	≥80.0%	Greagent Chemical reagent
Sodium hydroxide	≥96.0%	Greagent Chemical reagent
Sodium sulfide nonahydrate	≥98.0%	Greagent Chemical reagent
Ammonium citrate tribasic	≥98.5%	Greagent Chemical reagent
Ammonium dihydrogen phosphate	≥99.0%	Greagent Chemical reagent
Sodium citrate dihydrate	≥99.0%	Greagent Chemical reagent
Glycerol	≥99.0%	Greagent Chemical reagent
Oxalic acid	≥99.0%	Greagent Chemical reagent

1-Propanol	≥99.5%	Greagent Chemical reagent
N,N-Dimethylformamide	≥99.5%	Greagent Chemical reagent
Ethanol	≥99.7%	Greagent Chemical reagent
Nickel(II) chloride hexahydrate	≥98.0%	Accela Chemical reagent
HCl	36.0-38.0 wt%	Fengchuan Reagent Technology Co., Ltd.

2.2. Preparation of NADESs

Table S2. Preparation of NADESs[a]

HBA		Betaine Hydrochloride			Choline Chloride		
Type	HBD	Proportion[b]	Phase separation capability	Extraction rate (%)	Proportion[b]	Phase separation capability	Extraction rate (%)
Acids	Acetic acid Glacial	1:1:0	Poor	—	1:1:0	Poor	—
	Oxalic acid	1:1:2	Poor	—	1:1:2	Poor	—
	Propionic acid	1:1:0	Ordinary	93.6	1:1:0	Ordinary	93.9
	Malonic acid	1:1:2	Poor	—	1:1:2	Poor	—
	Lactic acid	1:1:0	Fine	96.4	1:1:0	Fine	96.2
	Butyric acid	1:1:0	Ordinary	93.1	1:1:0	Ordinary	94.5
	DL-Malic acid	3:2:6	Poor	—	1:1:2	Poor	—
	Sorbic acid	1:1:2	Poor	—	1:1:2	Poor	—
	Itaconic acid	1:1:2	Poor	—	1:1:2	Poor	—
Alcohols	Methyl alcohol	1:1:0	Poor	—	1:1:0	Poor	—
	Ethanol	1:3:0	Poor	—	1:4:0	Poor	—
	Ethylene glycol	1:2:0	Ordinary	88.6	1:1:2	Ordinary	89.4
	1-Propanol	1:1:0	Poor	—	1:1:0	Poor	—
	1,3-Propanediol	1:4:0	Ordinary	89.8	1:4:0	Ordinary	90.8
	2-Propanol	1:1:0	Poor	—	1:1:0	Poor	—
	Glycerol	1:2:1	Poor	—	1:2:1	Poor	—
	1-Butanol	1:1:0	Poor	—	1:4:0	Poor	—
	Xylitol	2:1:8	Poor	—	1:1:1	Fine	96.1
Sugars	D-(+)-Glucose	1:1:4	Poor	—	1:1:4	Poor	—
	D-(-)-Fructose	2:1:2	Poor	—	1:1:4	Poor	—

[a] [NADES] ≈ 25.0 wt%; $[K_3PO_4]$ ≈ 40.0 wt%; $[Au(S_2O_3)_2^{3-}]$ = 200 mg·L^{-1}; pH = 10; T = 298.15 K; t = 20 min.

[b] Refers to the molar ratio of HBA, HBD, and water.

2.2. Preparation of NADESs

Characterization of NADESs: ^{1}H NMR analysis results

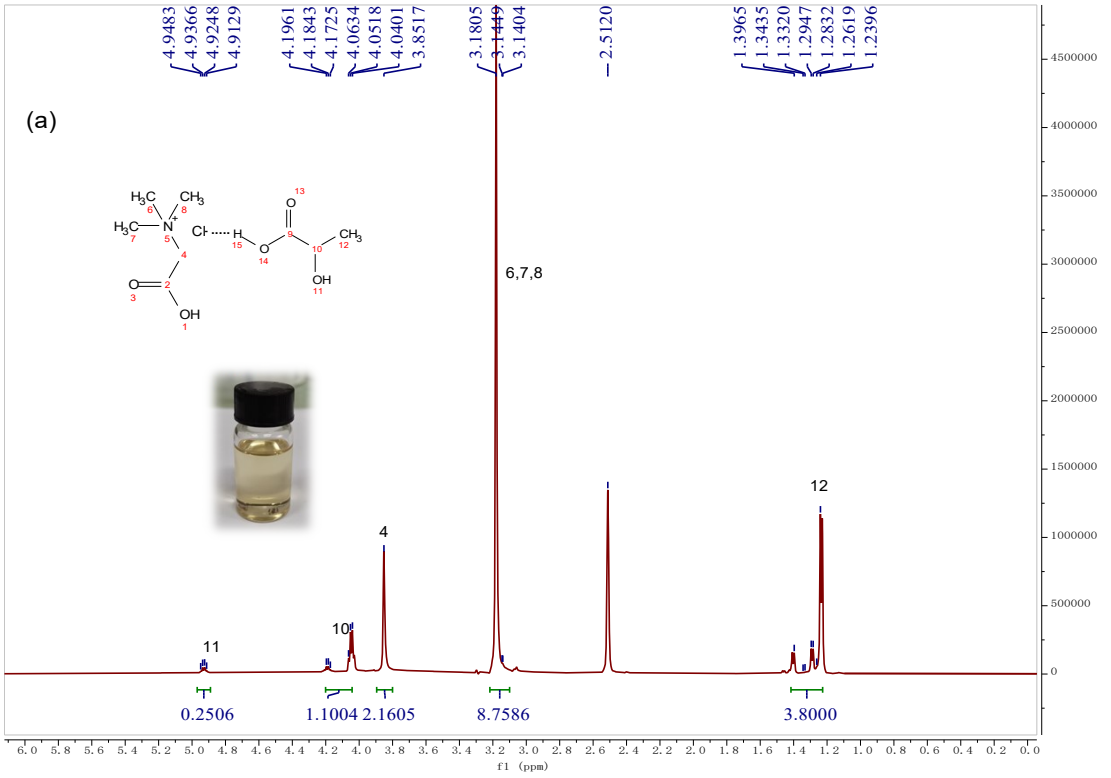

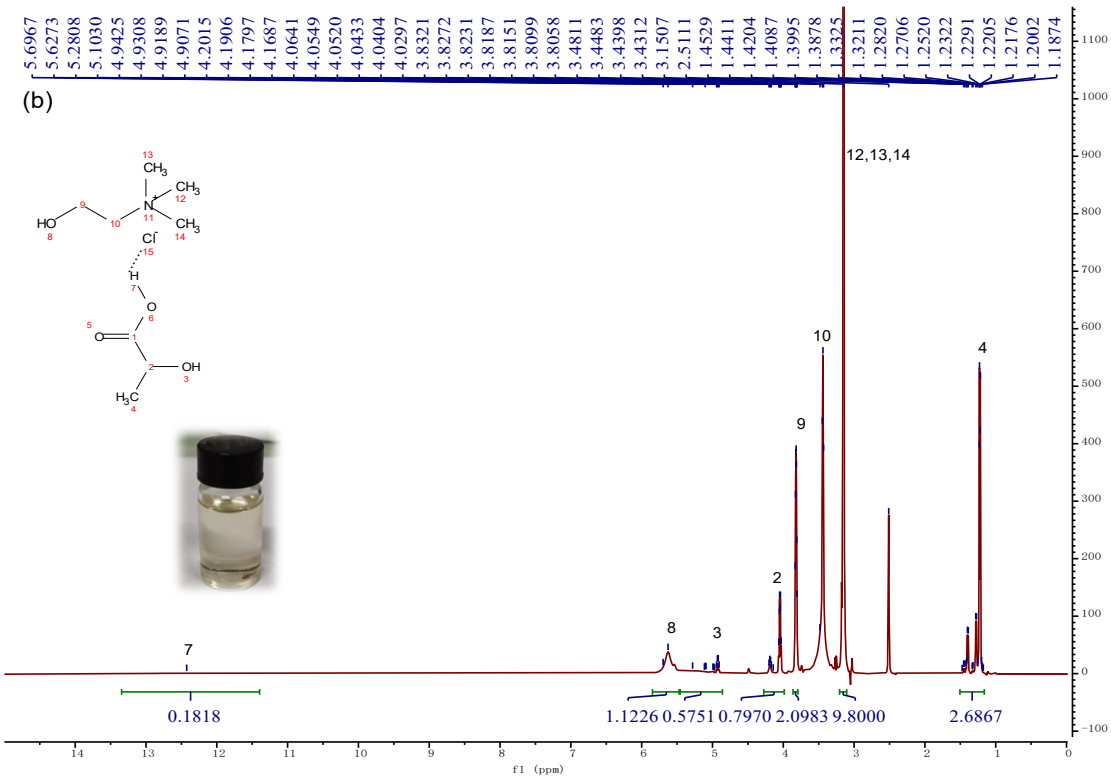

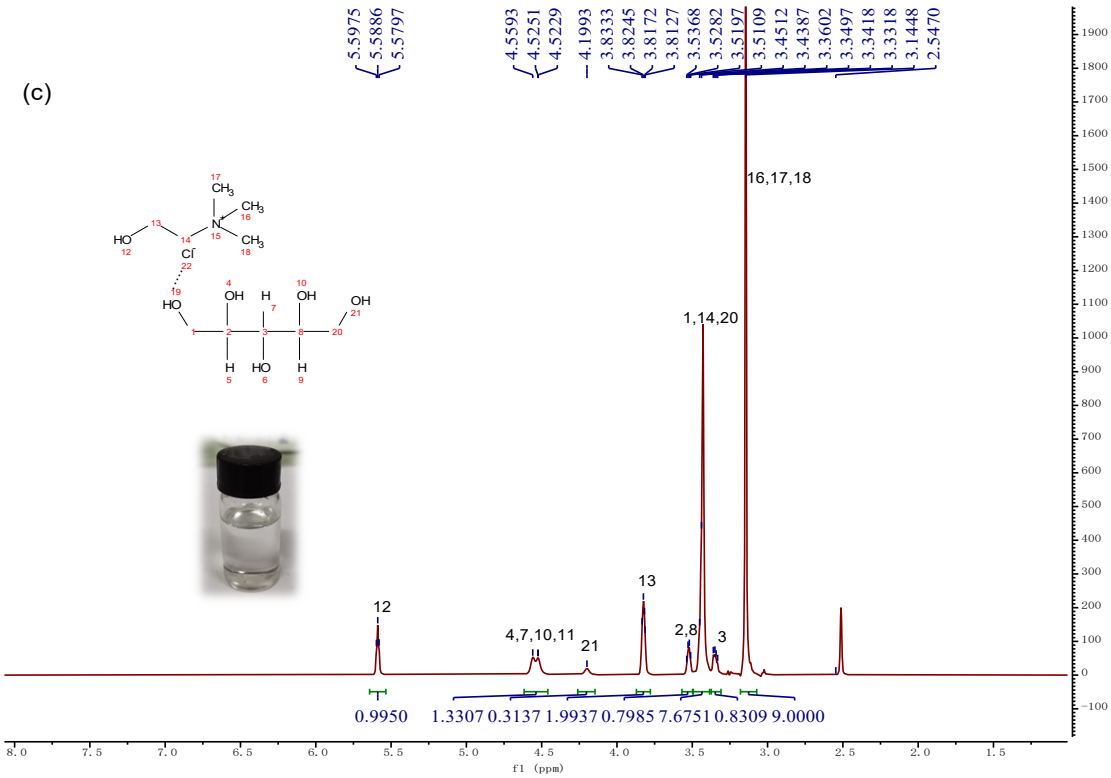

Fig. S1. (a)~(c) represent ^{1}H NMR spectra of Bet-Lac, ChCl-Lac and ChCl-Xyl with DMSO-d6 as the solvent, respectively

Table S3. ^{1}H NMR data of Bet-Lac, ChCl-Lac and ChCl-Xyl. (600 MHz, DMSO-d6).

Name	^{1}H NMR (ppm)
Bet-Lac	δ 4.9306 (q, J = 7.1 Hz, 1H), 4.0518 (m, 1H), 3.8517 (s, 2H), 3.1805 (s, 9H), 1.2672 (m, 3H).
ChCl-Lac	δ 12.4255 (s, 1H), 5.6273 (s, 1H), 4.9960 (m, 1H), 4.0474 (m, 1H), 3.8210 (tt, J = 5.3, 3.0 Hz, 2H), 3.4398 (t, J = 5.1 Hz, 2H), 3.1507 (s, 9H), 1.2363 (m, 3H).
ChCl-Xyl	δ 5.5886 (t, J = 5.3 Hz, 1H), 4.5358 (m, 4H), 4.1993 (s, 1H), 3.8250 (t, J = 4.8 Hz, 2H), 3.5239 (q, J = 5.2 Hz, 2H), 3.4450 (d, J = 7.5 Hz, 6H), 3.3459 (dd, J = 10.9, 6.2 Hz, 1H), 3.1448 (s, 9H).

Characterization of NADESs: FT-IR analysis

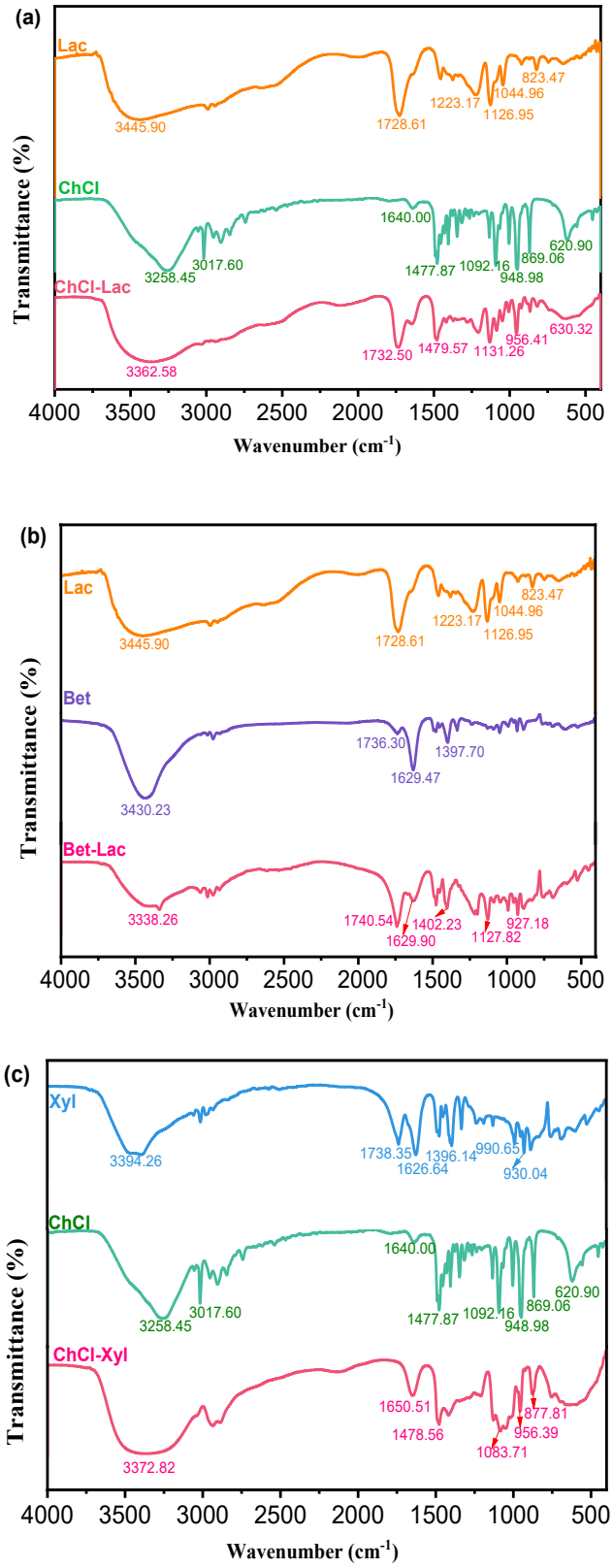

Fig. S2. FT-IR spectra of pure substances ChCl-Lac (a), Bet-Lac (b) and ChCl-Xyl (c).

TEXT S1. FT-IR analysis of NADESs

To study the interaction between the HBA (Bet or ChCl) and HBD (Lac or Xyl), the raw materials and synthesized compounds were characterized using FT-IR. In the FT-IR spectrum of pure Lac (Fig. S2a), there is a broad peak at 3445.90 cm^{-1} that corresponds to the -OH stretching vibration. After ChCl-Lac formed, the -OH absorption band was dispersed and wider; also, the frequency was redshifted to 3362.58 cm^{-1}.[1] These results indicate that the -OH in the carboxyl group forms an intermolecular hydrogen bond with the chloride in ChCl.[2] Furthermore, the stretching vibration peak of C=O is at 1728.61 cm^{-1} in the spectrum of pure Lac. After ChCl-Lac was generated, the stretching vibration peak of C=O shifted to 1732.50 cm^{-1} ($\Delta\lambda \approx 4$ cm^{-1}). The reason for this is that the generation of intermolecular hydrogen bonds causes the electron cloud between the atoms in the C=O bond, which was originally close to the O atom, to move to a certain extent toward the C atom, thus affecting the tensile vibration of C=O. Bet-Lac and ChCl-Xyl have similar results; details are provided in Fig. S2b and c. These FT-IR results confirm that the HBAs and HBDs proposed in this work successfully formed NADESs through hydrogen bonds.

2.4. Extraction procedures

TEXT S2. Preparation of the stock solution of $Au(S_2O_3)_2^{3-}$

Preparation of gold thiosulfate $[Au(S_2O_3)_2]^{3-}$: First, pure gold was dissolved in aqua regia on a heating plate, followed by nitrate removal with 6 $mol \cdot L^{-1}$ HCl for 3 times. Thereafter, the gold solution was dissolved to 2 $g \cdot L^{-1}$ with deionized water and adjust the pH value of the solution to 9.0. Then add 1.0 $mol \cdot L^{-1}$ $Na_2S_2O_3$ solution into the above gold solution until the solution becomes colorless [3]. Finally, the solution was diluted to 200 $mg \cdot L^{-1}$ with deionized water and adjusting the pH to 9.0 for standby.

Table S4. Distribution ratio of NADES + K_3PO_4 + water system at extraction equilibrium [c]

Distribution ratio		NADES		
		Bet-Lac	ChCl-Lac	ChCl-Xyl
Concentration of gold (mg/L)	5.00	/	/	/
	10.00	/	/	/
	25.00	/	/	/
	50.00	79.91±4.37	/	97.61±2.86
	100.00	39.82±1.99	64.79±3.30	87.36±1.97
	200.00	24.17±0.57	28.31±0.82	79.31±2.45
	500.00	19.09±1.63	22.841.07±	60.04±3.84
	900.00	18.13±0.88	21.96±1.57	55.48±1.93
Time (min)	1.00	16.19±0.75	22.35±1.50	40.61±2.32
	3.00	17.12±2.79	23.68±2.87	43.14±2.58
	5.00	17.22±3.18	23.71±1.61	43.84±0.80
	10.00	17.52±1.56	24.23±2.32	65.11±2.24
	15.00	17.62±2.40	24.46±3.27	72.52±1.38
	20.00	17.72±0.57	24.34±0.71	79.31±2.45
pH	7.00	6.62±0.32	9.32±0.90	14.91±0.24
	8.00	10.21±0.77	14.14±0.83	30.29±3.23
	9.00	17.72±0.57	24.34±0.71	79.31±2.45
	10.00	10.06±2.94	14.07±1.86	33.21±2.62
	11.00	8.41±1.12	11.76±1.21	17.60±1.28
	12.00	7.43±0.43	10.39±0.87	15.31±0.89
	13.00	6.18±0.45	8.68±0.52	12.82±0.56
	14.00	5.77±0.65	8.10±0.43	11.91±0.39
T(K)	298.15	17.72±0.57	24.34±0.71	79.31±2.45
	303.15	19.30±0.23	26.48±0.83	80.93±0.85
	313.15	22.57±1.35	31.06±2.71	86.38±1.93
	323.15	25.14±2.02	34.59±2.38	92.57±2.20
	333.15	29.40±0.52	39.03±1.98	99.63±0.00
Selectivity of NADES-ATPSs for $Au(S_2O_3)_2^{3-}$	$[Au(S_2O_3)_2]^{3-}$	21.54±0.78	23.01±1.57	73.26±2.56
	$[Cu(NH_3)_4]^{2+}$	0.00	0.00	0.00
	$[Ni(NH_3)_6]^{2+}$	0.06±0.01	0.00	0.39±0.02
	$[Co(NH_3)_6]^{3+}$	0.11±0.01	0.09±0.02	0.48±0.03

[c] $SD = (\sum_{i=1}^{n}(X_{exp} - X_{ave})^2/(n-1))^{0.5}$, where X_{exp} and X_{ave} represent the experimental and average values of the distribution coefficient respectively, and n represents the number of samples.

TEXT S3. Preparation of MoS_2

In this work, we obtained layered nanosheets MoS_2 based on a rapid microwave-assistant solvothermal synthesis method. First, add ammonium molybdate(VI) tetrahydrate (4 mmol) and thiourea (60 mmol) into 50 ml of deionized water and stir evenly at room temperature. Then, the solution was transferred to a 100 mL reaction tank and heated in a microwave reactor (UWave-2000) at a microwave power of 400 W at 200°C for 120 minutes. After synthesis, it was washed three times with deionized water and separated by centrifuge (8000 rpm, 10 minutes). The synthesized MoS_2 was dried in a vacuum drying oven at 80 °C for 24 hours and then stored for use.

3.3. Correlation of binodal curve and tie-line.

Table S5. Fitting parameters of NADES + K_3PO_4 + water system

	a	b	c	d	R^2	SD[d]
Bet-Lac	163.8657	-48.7758	4.6932	-0.0180	0.9987	0.1056
ChCl-Lac	145.9355	-46.9527	5.0954	-0.0247	0.9963	0.4665
ChCl-Xyl	213.2084	-46.4719	2.0229	0.0109	0.9985	0.1769

[d] $SD = (\sum_{i=1}^{n}(w_N^{cal} - w_N^{exp})^2/N)^{0.5}$, where w_N^{cal} and w_N^{exp} represent the calculated and experimental values of the mass fraction of NADES respectively, and N represents the number of double nodes.

Table S6. Tie-line data of NADES + K_3PO_4 + water system [e]

	Total system		Bottom phase			Top phase			S	TLL
	K(A)	N(A)	K(B)	N(B)	W(B)	K(T)	N(T)	W(T)		
Bet-Lac	35.00	25.00	48.83	9.37	41.80	9.70	48.24	42.06	-0.99	55.15
ChCl-Lac	32.50	25.00	45.77	9.71	44.52	6.42	50.23	43.35	-1.03	56.48
ChCl-Xyl	40.00	25.00	38.86	18.63	42.51	10.52	52.15	37.33	-1.18	43.89

[e] where K, N, and W represent the mass fraction (wt%) of K_3PO_4, NADES, and water respectively, and A, T, and B represent all, the top and bottom phases respectively.

3.4. Optimization of the extraction by NADESs

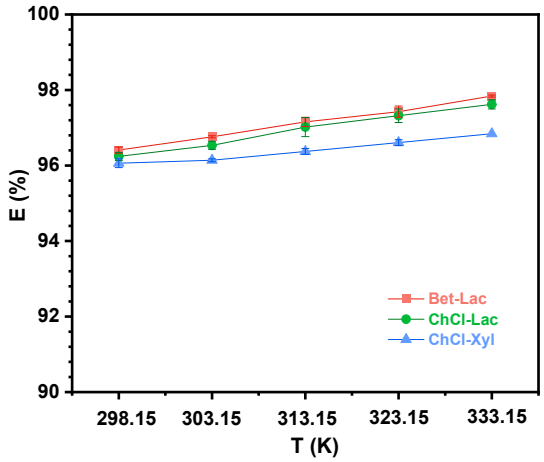

Fig. S3. Effects of temperature on extraction of $Au(S_2O_3)_2^{3-}$ under the conditions of [ChCl-Lac] ≈ 25.0 wt%, $[K_3PO_4]$ ≈ 32.5 wt%, [Au(I)] = 200 mg·L^{-1}, pH = 9.0 and time = 20 min.

Table S7. Thermodynamic parameters of extraction of $Au(S_2O_3)_2^{3-}$ by NADES-ATPSs

T(K)	NADES-ATPS	ΔG_m^0(kJ·mo^{l-1})	ΔH_m^0(kJ·mol^{-1})	ΔS_m^0(J·mol^{-1} K^{-1})	T×ΔS_m^0(kJ·mol^{-1})
298.15		-10.91±0.38			18.80±0.38
303.15		-11.23±0.39			19.11±0.39
313.15	Bet-lac	-11.86±0.40	11.66±0.40	63.04±1.29	19.74±0.40
323.15		-12.49±0.42			20.37±0.42
333.15		-13.12±0.43			21.00±0.43
298.15		-10.74±0.38			18.99±0.38
303.15		-11.06±0.38			19.31±0.38
313.15	ChCl-lac	-11.70±0.39	11.05±0.39	63.70±1.26	19.95±0.39
323.15		-12.34±0.41			20.58±0.41
333.15		-12.97±0.42			21.22±0.42
298.15		-8.53±0.28			16.25±0.28
303.15		-8.80±0.28			16.52±0.28
313.15	ChCl-Xyl	-9.34±0.29	5.44±0.29	54.51±0.93	17.07±0.29
323.15		-9.89±0.30			17.62±0.30
333.15		-10.43±0.31			18.16±0.31

3.6. Characterization of NADES-rich phase loaded with Au(I).

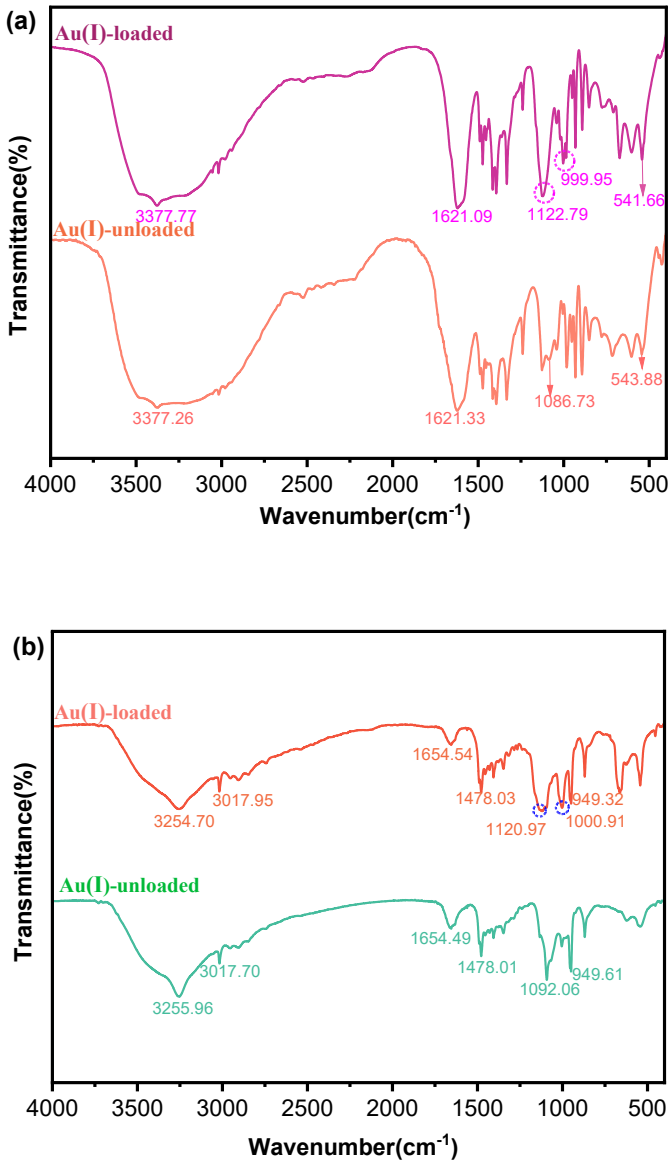

Fig. S4. FT-IR spectra of Bet-Lac (a) and ChCl-Xyl (b) before and after loaded with Au(I)

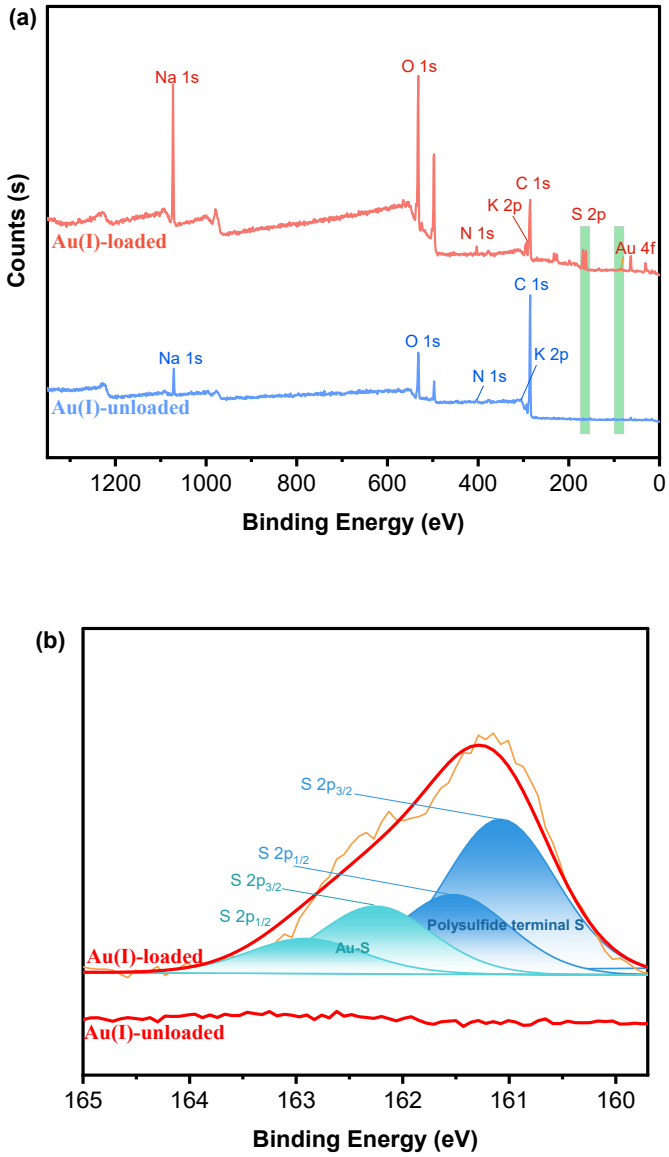

Fig. S5. Wide scanning XPS spectra (a) and S 2p spectra (b) of the NADES-rich phase with or without Au(I) loaded.

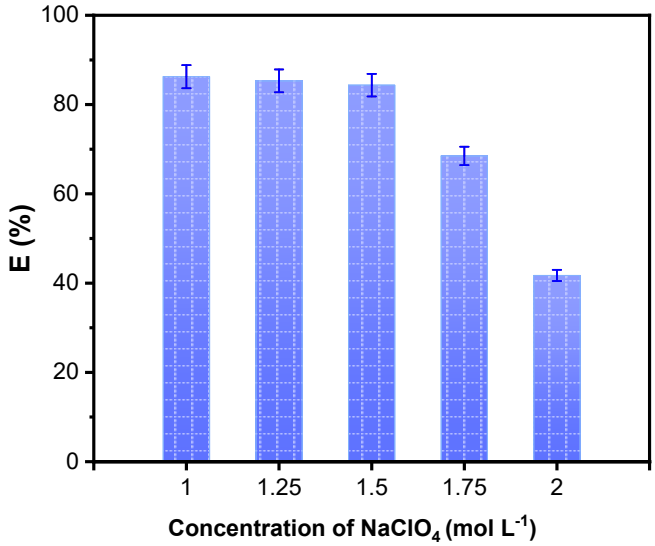

Fig. S6. Effects of ClO_4^- content on extraction efficiency under the conditions of [ChCl-Lac] =25.0 wt%, [K_3PO_4]=32.5 wt%, [Au(I)] = 200 mg·L^{-1}, pH = 9.0, T = 298.15 K and t = 20 min.

TEXT S4. Characterization of MoS_2

XRD analysis. 2H MoS_2 usually exhibits a poor electrochemical performance due to limited active sites and intrinsic poor electrical transport property.[4] Moreover, MoS_2 tends to form a stable 2H phase by restacking during the process of synthesis due to a thermodynamically metastable 1T phase.[5, 6] In addition, compared with 2H phase MoS_2, metallic 1T phase MoS_2 can promote both ion diffusion and electron transport due to the higher conductivity and the large number of edge active sites of 1T-MoS_2 that can accelerate the redox kinetics of polysulfides.[7-9]

Compared with traditional hydrothermal methods, microwave-assistant solvothermal synthesis method has fast, uniform, and efficient heating;[10] thus, the resulting MoS_2 has more active sites and intrinsic activity. MoS_2, generally in the form of semiconductor phase (2H), but when ion migration occurs, it can be converted into metastable metal phase (1T). To obtain MoS_2 with high catalytic efficiency, we use a rapid microwave-assistant solvothermal synthesis method to convert part of the inert 2H phase into the catalytically active 1T phase. The prepared MoS_2 nanomaterial was characterized by XRD, as shown in Fig. S7. The characteristic diffraction peaks observed at 2θ = 9.1° and 18.2° of the sample correspond to the crystal plane (002) and crystal plane (004) of 1T-MoS_2 respectively.[11, 12] The diffraction peaks at 2θ = 32.5°, 35.8° and 57.8° correspond to the (100),

(102) and (110) crystal planes of 2H-MoS_2 (JCPDS card No. 73-1508),[13] respectively. This indicates the presence of a thermodynamically unstable 1T phase in the final product under the rapid synthesis of microwave-assistant solvothermal synthesis method. The final product is amorphous MoS_2 with 1T phase and 2H phase coexistence. The absence of the 002 diffraction at 2θ = 14.4° suggests that absence of stacking, thus the sample should be an aggregate of single sheets of MoS_2.[14] This proves that an amorphous phase of MoS_2 is formed.[15]

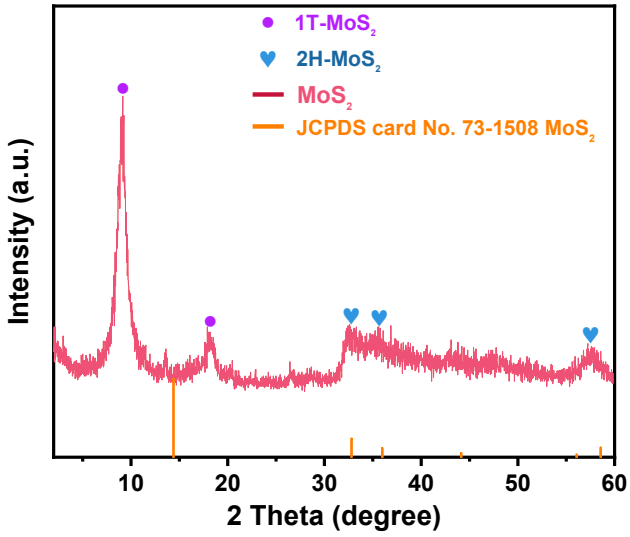

Fig. S7. XRD patterns of MoS_2 that were synthesized using a microwave-assisted method.

3.8. Reduction mechanism of MoS_2

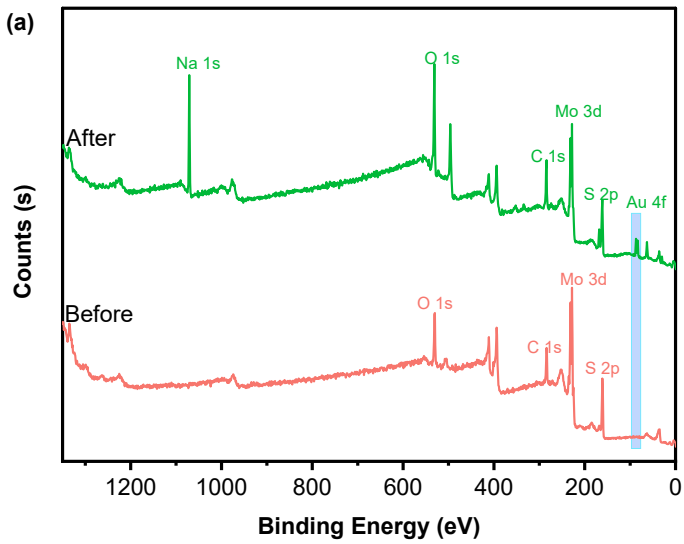

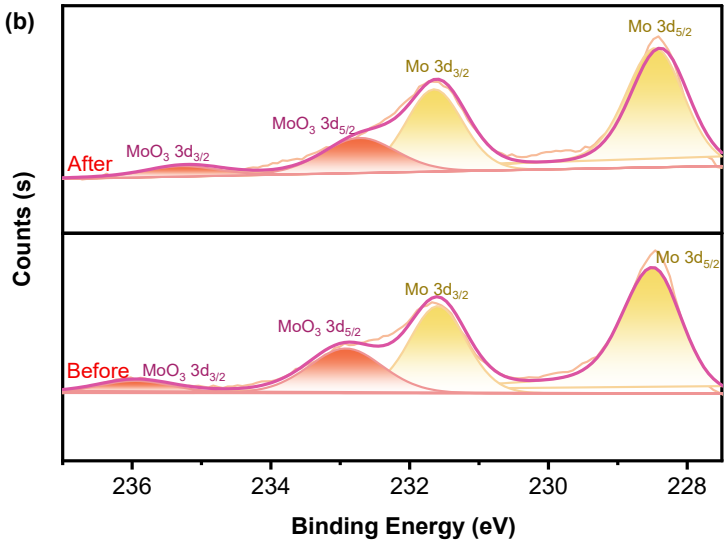

Fig. S8. Wide scanning XPS spectra (a) and Mo 3d spectra (b) of sediments before and after reduction

TEXT S5. Mechanism of gold recovery from NADES-rich phase by MoS_2

UV–vis diffuse reflectance spectroscopy (DRS) of MoS_2 is presented in Fig. S9a. MoS_2 shows excellent absorption properties in both the ultraviolet and visible light regions because of the quantum effect of the transverse size of MoS_2. This is consistent with the value that was obtained by Ghaleghafi et al. [16] and is very different from MoS_2 with good crystallization. This further confirms the high disorder of the quasi-amorphous phase of MoS_2. The bandgap (E_g) of semiconductors can be obtained according to the tauc plot method [17], which uses Eq. (S1).

$$(\alpha hv)^{\frac{1}{n}} = A\left(hv - E_g\right) \qquad \text{(S1)}$$

Here, α, h, v, A, and E_g are the absorbance, Planck's constant, the optical frequency, a constant, and the semiconductor bandgap, respectively. The index n is related to the type of semiconductor that is used. For the indirect bandgap semiconductor MoS_2, the index n is 2. The value of E_g for MoS_2 was obtained from Fig. S9b and is 1.66 eV. This is consistent with the value that was obtained by Zeng et al. [18]. In addition, other essential parameters (the photocatalytic reaction, conduction

band energy (E_{CB}), and valence band energy (E_{VB})) can be calculated using Eqs. (S2)-(S4) [19].

$$E_{CB} = X - E_e - 0.5E_g \quad \text{(S2)}$$

$$E_{VB} = E_g + E_{CB} \quad \text{(S3)}$$

$$\chi = [\chi(Mo)^a \chi(S)^b]^{1/(a+b)} \quad \text{(S4)}$$

χ represents the Mulliken electronegativity of the semiconductor MoS_2; a and b refer to the atomic numbers of Mo and S in MoS_2, respectively. E_e, E_{CB}, and E_{VB} are the energy of free electrons and hydrogen (4.5 eV), the conduction band, and the valence band of MoS_2, respectively. According to ref. [20], the values of χ(Mo) and χ(S) are 3.90 and 6.22, respectively. From the above equations, the value of χ for MoS_2 is 5.32, and the values of E_{CB} and E_{VB} are -0.01 eV and 1.65 eV, respectively.

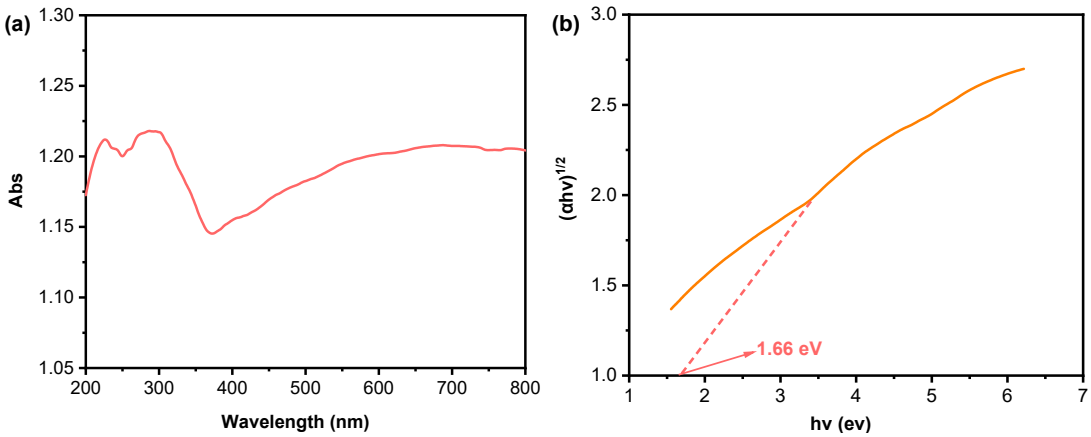

Fig. S9. Diffuse reflection absorption curve of MoS_2 (a) and Tauc plots of MoS_2 (b)

TEXT S6. Construction of a cyclic model

First, according to method 2.4, $Au(S_2O_3)_2^{3-}$ was extracted from the solution using ChCl-Lac-ATPS. After separating the salt-rich and NADES-rich phases, defect-rich MoS_2 was added to the NADES-rich phase for the photocatalytic reduction of $Au(S_2O_3)_2^{3-}$. After centrifugal separation, the NADES-rich phase was washed with 40.0 wt% K_3PO_4 solutions to regenerate NADES. The gold-

loaded sediment was eluted with 1.0 mol·L^{-1} Na_2S solution at room temperature for three hours (the elution rate reached 99.9%) and then centrifuged to separate the sediment. The sediment was washed with ultrapure water and ethanol and dried in a vacuum drying oven at 60 °C for 24 hours. Then, the regenerated ChCl-Lac and MoS_2 were repeatedly used to extract and reduce Au(I). It is worth noting that, the salt addition during cyclic extraction comes from the salt-rich salt content in the phase diagram.

TEXT S7. The calculation details

Computing software:

Structure optimization frequency calculation: Gauss 09 electrostatic potential: Multiwfn 3.8.

Computing level: b3lyp/6-311G* (C, H, P, N, Cl) SDD (Au) scrf=(smd, solvent=water) em=gd3bj.

Au is optimized using pseudopotential basis set SDD [21, 22], S, O, C, N, and H adopt a 6-311G(d) foundation set. The electrostatic potential of the local surface (ESP) is generated by the Mutiwfn 3.8 program (the isosurface is defined as the electrostatic potential of 0.002au) [23].

$Au(S_2O_3)_2^{3-}$

-3 1

Au	-0.00001600	-0.72619300	-0.00001500
S	3.06895900	0.82909800	0.16774000
S	-3.06886700	0.82914100	-0.16769400
S	2.15091100	-0.75110200	-0.94142200
S	-2.15099600	-0.75124100	0.94141300
O	3.07743600	0.43486400	1.60845400
O	4.44586600	0.92213100	-0.40128700
O	2.27527100	2.07255700	-0.06388500
O	-2.27517000	2.07259300	0.06396400
O	-3.07746000	0.43494300	-1.60841900
O	-4.44579800	0.92228000	0.40124700

Zero-point correction= 0.028364 (Hartree/Particle)

Thermal correction to Energy= 0.041568

Thermal correction to Enthalpy= 0.042512

Thermal correction to Gibbs Free Energy= -0.016426

Sum of electronic and zero-point Energies= -2180.604578

Sum of electronic and thermal Energies= -2180.591374

Sum of electronic and thermal Enthalpies= -2180.590430

Sum of electronic and thermal Free Energies= -2180.649368

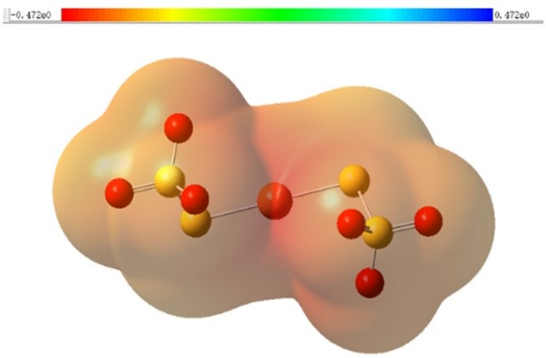

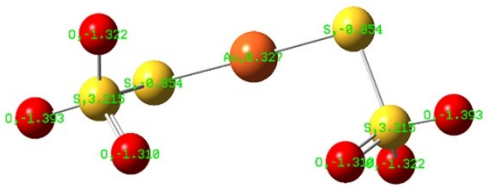

Choline chloride

0 1

C	-2.62173300	-0.67328600	-0.02163400
C	-1.71876700	0.55688800	-0.03434200
N	-0.23238200	0.28371000	-0.01801200
C	0.47880000	1.60447200	-0.08135000
O	-3.97856300	-0.23024000	-0.03465600
C	0.18019600	-0.54040300	-1.20209100
C	0.17605100	-0.41848300	1.24418800
H	-2.49298200	-1.27251100	-0.92195900
H	-2.43269400	-1.30605800	0.84876200
H	-1.91651200	1.14460200	-0.92975300
H	-1.92461500	1.17234900	0.84200200
H	1.55024300	1.41554900	-0.06036000
H	0.19674400	2.10480100	-1.00499300
H	0.17842500	2.20043000	0.77756800
H	-4.17126100	0.16822400	0.82320000
H	-0.26106600	-1.53004900	-1.12296800
H	-0.16330300	-0.04257400	-2.10619200
H	1.26571400	-0.61787100	-1.19463400
H	-0.27186500	-1.40749800	1.26756100
H	1.26111900	-0.50232100	1.24440700
H	-0.16323300	0.17181500	2.09248400
Cl	3.75489300	-0.29518100	0.02468100

Zero-point correction= 0.198944 (Hartree/Particle)

Thermal correction to Energy= 0.210227

Thermal correction to Enthalpy= 0.211171

Thermal correction to Gibbs Free Energy= 0.160565

Sum of electronic and zero-point Energies= -789.096104

Sum of electronic and thermal Energies= -789.084821

Sum of electronic and thermal Enthalpies= -789.083877

Sum of electronic and thermal Free Energies= -789.134483

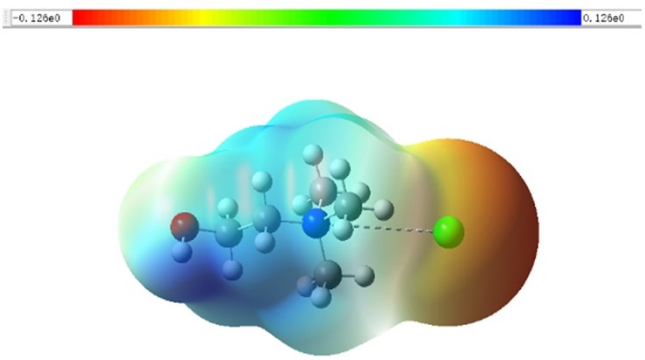

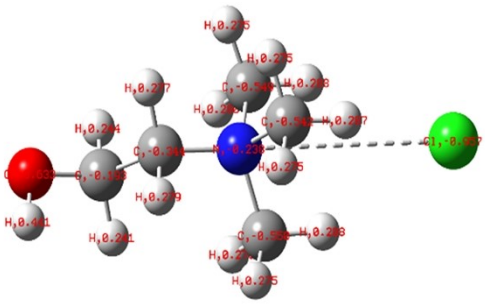

Lactic acid

0 1

O	1.30942800	0.98338200	-0.45492100
C	0.80163000	-0.12967700	0.09360000
C	-0.68854200	-0.04111600	0.39824400
C	-1.44457700	-1.05564500	-0.44942700
O	-1.24425900	1.24050700	0.14418000
O	1.46575500	-1.11851500	0.32816000
H	2.25895200	0.84647700	-0.61053500
H	-0.78840200	-0.30289700	1.45830300
H	-1.05724500	-2.06066800	-0.28165300
H	-2.50216100	-1.03735000	-0.18150200
H	-1.34576200	-0.81046400	-1.50972800
H	-0.82384600	1.88054100	0.73126600

Zero-point correction= 0.095074 (Hartree/Particle)
Thermal correction to Energy= 0.101722
Thermal correction to Enthalpy= 0.102666
Thermal correction to Gibbs Free Energy= 0.064425
Sum of electronic and zero-point Energies= -343.633160
Sum of electronic and thermal Energies= -343.626512
Sum of electronic and thermal Enthalpies= -343.625568
Sum of electronic and thermal Free Energies= -343.663809

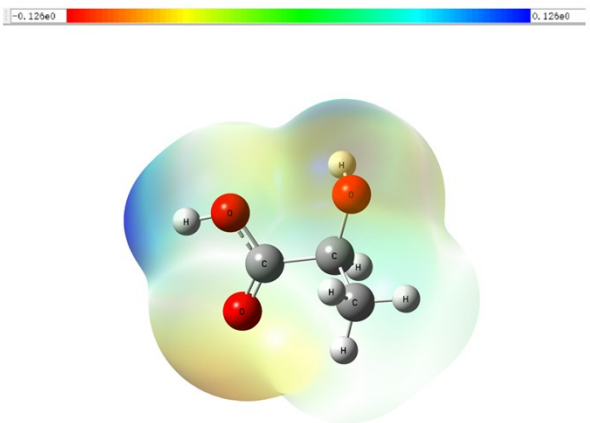

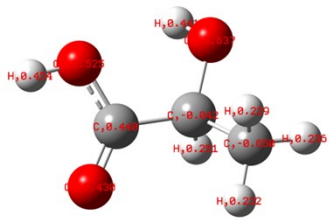

Chlorine

-1 1

Cl	0.00000000	0.00000000	0.00000000

Zero-point correction=	0.000000 (Hartree/Particle)
Thermal correction to Energy=	0.001416
Thermal correction to Enthalpy=	0.002360
Thermal correction to Gibbs Free Energy=	-0.015023
Sum of electronic and zero-point Energies=	-460.406331
Sum of electronic and thermal Energies=	-460.404915
Sum of electronic and thermal Enthalpies=	-460.403971
Sum of electronic and thermal Free Energies=	-460.421354

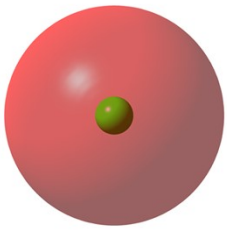

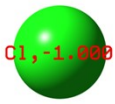

Choline Chloride - Lactic acid

0 1

C	-2.62094100	-0.67533800	-0.02151900
C	-1.71989000	0.55623000	-0.03588200
N	-0.23291800	0.28559500	-0.01777000
C	0.47569400	1.60741500	-0.08364200
O	-3.97837500	-0.23410800	-0.03536600
C	0.18198400	-0.54055200	-1.19956100
C	0.17567900	-0.41292800	1.24636900
H	-2.49118100	-1.27572600	-0.92092100
H	-2.43122600	-1.30651700	0.84987200
H	-1.91781100	1.14187400	-0.93261200
H	-1.92735600	1.17309500	0.83908800
H	1.54756200	1.42109200	-0.06132600
H	0.19353200	2.10495500	-1.00875400
H	0.17334700	2.20490900	0.77350700
H	-4.17171700	0.16521300	0.82195100
H	-0.25841400	-1.53044800	-1.11878000
H	-0.16091900	-0.04510300	-2.10519900
H	1.26758100	-0.61705900	-1.19041300
H	-0.27166200	-1.40212700	1.27220600
H	1.26078900	-0.49638100	1.24696600
H	-0.16411800	0.17933800	2.09307700
Cl	3.75610900	-0.29719900	0.02435600
O	9.71374378	-0.05550170	0.17643408
C	10.18214010	-1.19866199	-0.34455045
C	11.69392126	-1.21524224	-0.53298242
C	12.30823133	-2.28660023	0.35820714
O	12.31789676	0.02165047	-0.22204858
O	9.46962983	-2.13587861	-0.64091814
H	8.74771517	-0.12496408	0.25717128
H	11.85660614	-1.47691111	-1.58526063
H	11.86467190	-3.26021402	0.14945693
H	13.38198725	-2.34248729	0.17239189
H	12.14538767	-2.04156468	1.41061203
H	11.99062669	0.69380810	-0.83209589

Zero-point correction= 0.294623 (Hartree/Particle)

Thermal correction to Energy= 0.314287

Thermal correction to Enthalpy= 0.315231

Thermal correction to Gibbs Free Energy= 0.241866

Sum of electronic and zero-point Energies= -1132.740379

Sum of electronic and thermal Energies= -1132.720714

Sum of electronic and thermal Enthalpies= -1132.719770

Sum of electronic and thermal Free Energies= -1132.793135

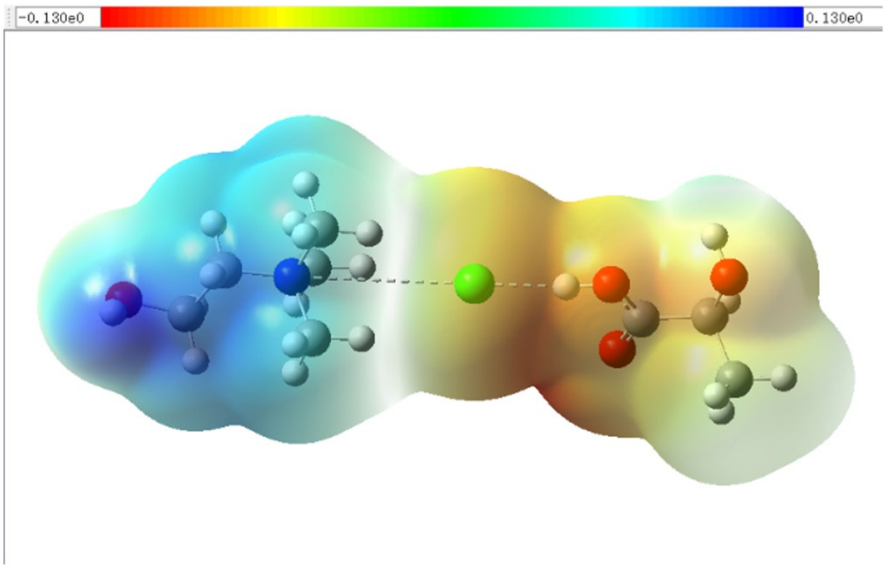
-0.130e0
0.130e0

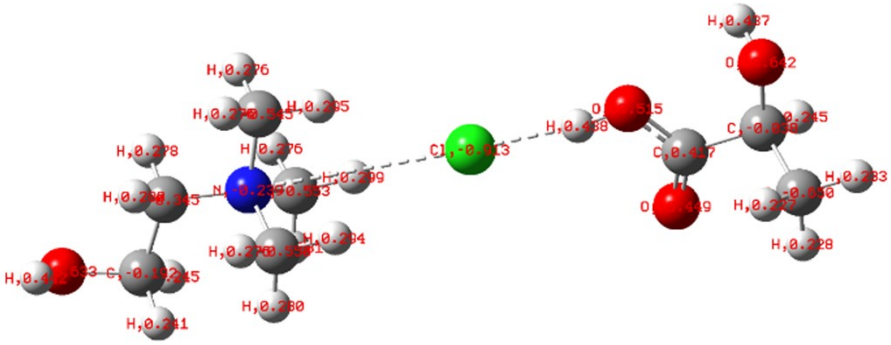

Choline Chloride - Lactic acid - $Au(S_2O_3)_2^{3-}$

0 1

Au	0.29020800	-1.27931300	0.19472100
S	3.16735000	-2.53542000	-1.27338600
S	-3.17480100	-1.43978400	0.20442500
S	2.22747700	-2.53163000	0.63843900
S	-1.64805000	-0.00176200	-0.16961000
O	-3.01381100	-2.56329200	-0.76447000
O	-3.04719600	-1.90033000	1.61924200
C	2.25332435	5.04423956	-3.36165004
C	3.12735451	4.52351635	-2.22342952
N	3.92050755	3.27224602	-2.52270990
C	4.74770454	2.95017274	-1.31298414
O	1.61204011	6.24060220	-2.92069828
C	4.84133739	3.48214691	-3.68933480
C	3.01001074	2.11497241	-2.80614989
H	2.85221900	5.32610745	-4.22641125
H	1.51122553	4.30707272	-3.67679544
H	3.84978522	5.28918921	-1.94425935
H	2.50668716	4.29282315	-1.35695645
H	5.33358560	2.05893644	-1.52229080
H	5.40489320	3.79218424	-1.10812162
H	4.08017476	2.77916750	-0.47161563
H	0.95231296	6.00082416	-2.25810101
H	4.25596695	3.62779176	-4.59221055
H	5.45645927	4.35655016	-3.48858986
H	5.45891147	2.59458970	-3.79423937
H	2.43339080	2.32763656	-3.69848680
H	3.61937519	1.22865491	-2.95357954
H	2.35017620	1.97794708	-1.95213206
C	-7.54155183	-0.40301034	6.59016673
C	-7.65503907	-0.30151283	5.07105562
N	-6.36315352	-0.46069225	4.29914291
C	-6.69201402	-0.38697251	2.83570619
O	-8.84362245	-0.22328556	7.14621540
C	-5.72503991	-1.78918144	4.58149778
C	-5.39941374	0.64175800	4.62878669
H	-7.21709408	-1.39539983	6.89993079
H	-6.84535387	0.33447927	6.99596733
H	-8.33188985	-1.07289492	4.70649907
H	-8.05458700	0.67497339	4.79537724
H	-5.76985712	-0.49428947	2.27086870
H	-7.38096153	-1.19278552	2.59383044

H	-7.15146331	0.57741735	2.63165811
H	-9.09393271	0.70200369	7.03155464
H	-5.38988354	-1.81746668	5.61421130
H	-6.45740164	-2.57185707	4.39697091
H	-4.87309850	-1.90234422	3.91663553
H	-5.09471021	0.55769314	5.66763651
H	-4.53274412	0.53868882	3.98111906
H	-5.89343923	1.59471182	4.45403016
C	-7.80942637	-5.88214505	-3.68574930
C	-6.62668749	-6.68042211	-3.14497866
N	-5.55875027	-5.87281357	-2.44386009
C	-4.51719127	-6.82732936	-1.93714717
O	-8.70897451	-6.79105043	-4.32004261
C	-6.13740632	-5.12588929	-1.27927053
C	-4.90128375	-4.90961011	-3.38914338
H	-8.37452524	-5.41312413	-2.88163500
H	-7.48948814	-5.10680599	-4.38586190
H	-6.98282718	-7.41540125	-2.42425266
H	-6.12948174	-7.20272700	-3.96287996
H	-3.74977839	-6.25677344	-1.42119851
H	-4.98905406	-7.52783756	-1.25318068
H	-4.09174781	-7.35691650	-2.78657105
H	-8.29743817	-7.10118042	-5.13649595
H	-6.81467553	-4.35917157	-1.64387142
H	-6.66999034	-5.83186178	-0.64638794
H	-5.32202198	-4.67078498	-0.72266264
H	-5.62523525	-4.16671520	-3.70861567
H	-4.07870297	-4.43076310	-2.86622517
H	-4.53051738	-5.46931963	-4.24513061
O	-4.44005400	-0.67248700	-0.02636100
O	3.32817800	-1.11436400	-1.71227900
O	4.48260900	-3.20012900	-1.02652900
O	2.31135800	-3.30908400	-2.21964100
O	7.99719703	-1.18925229	-4.47894651
C	7.65498088	-0.15997842	-5.26705746
C	8.66376323	0.13202085	-6.37085018
C	8.01752262	-0.10473149	-7.72942482
O	9.83273857	-0.67052673	-6.29775509
O	6.63613237	0.48289956	-5.11693989
H	7.30878127	-1.30351870	-3.80249863
H	8.91622219	1.19381976	-6.26561728
H	7.11621720	0.49900325	-7.83618770
H	8.71942497	0.16904453	-8.51871707
H	7.75321087	-1.15888867	-7.84347949

H	10.29126315	-0.47258454	-5.47214416
O	-0.21123423	-0.11047970	5.84798128
C	0.36822061	1.09848157	5.86472025
C	0.75188730	1.57788410	7.25907920
C	2.26548022	1.71813017	7.35273346
O	0.32953705	0.70415381	8.29548863
O	0.56919321	1.75389697	4.86276200
H	-0.42871346	-0.33689296	4.92820163
H	0.28532502	2.56389059	7.37015228
H	2.63740898	2.38931338	6.57850641
H	2.53330319	2.12517735	8.32904587
H	2.74328044	0.74244106	7.23502944
H	-0.63465280	0.66684191	8.29323821
O	-0.57215186	-6.13204585	-4.06133263
C	-0.03432914	-5.19264292	-4.85247377
C	0.91223388	-5.74669558	-5.90997453
C	0.34494775	-5.47406554	-7.29679209
O	1.13417853	-7.14445394	-5.79621594
O	-0.27650871	-4.00847381	-4.73857796
H	-1.15379341	-5.69708865	-3.41553069
H	1.85089748	-5.19433305	-5.78335432
H	0.16476428	-4.40791652	-7.43501507
H	1.05543595	-5.81135252	-8.05312963
H	-0.59603139	-6.01278537	-7.43264396
H	1.56339490	-7.32043722	-4.95012936

Zero-point correction=	0.915401 (Hartree/Particle)
Thermal correction to Energy=	0.983845
Thermal correction to Enthalpy=	0.984789
Thermal correction to Gibbs Free Energy=	0.802993
Sum of electronic and zero-point Energies=	-4197.815986
Sum of electronic and thermal Energies=	-4197.747541
Sum of electronic and thermal Enthalpies=	-4197.746597
Sum of electronic and thermal Free Energies=	-4197.928393

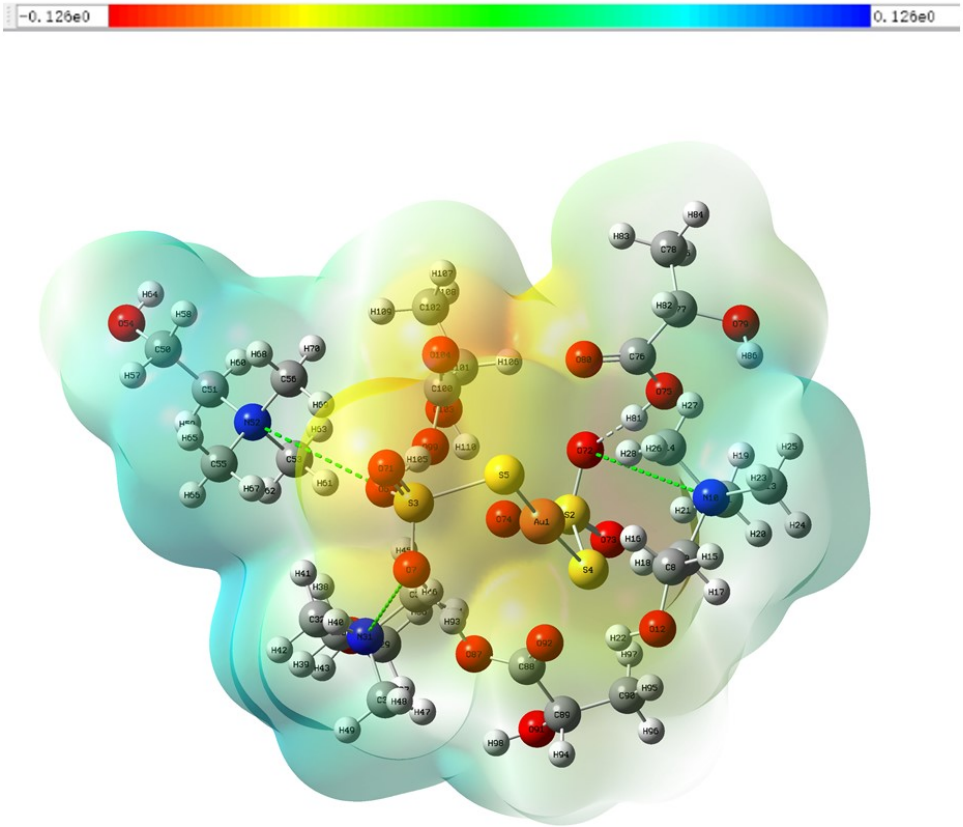
-0.126e0
0.126e0

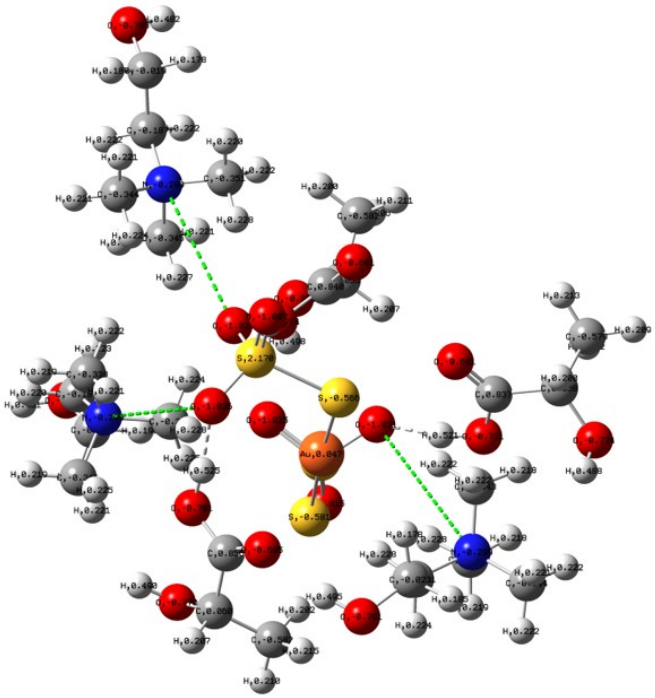

Reference

1. M. Shyama and S. Lakshmipathi, *Journal of Molecular Liquids*, 2020, **304**, 112720.
2. D. J. G. P. van Osch, L. F. Zubeir, A. van den Bruinhorst, M. A. A. Rocha and M. C. Kroon, *Green Chemistry*, 2015, **17**, 4518-4521.
3. H. Yu, F. Zi, X. Hu, Y. Nie, P. Xiang, J. Xu and H. Chi, *Hydrometallurgy*, 2015, **154**, 111-117.
4. S. Wu, Y. Ke, J. Tang, X. Lei, H. Deng and Z. Lin, *Surfaces and Interfaces*, 2022, **30**, 101869.
5. Q. Luo, M. Zhang, J. M. Liu, Z. W. Li, Y. Y. Hu, Y. H. Yin, X. B. Liu, Y. S. Li and Z. P. Wu, *Electrochimica Acta*, 2022, **413**, 140178.
6. N. Gao, Y. Zhang, C. Chen, B. Li, W. Li, H. Lu, L. Yu, S. Zheng and B. Wang, *Journal of Materials Chemistry A*, 2022, **10**, 8378-8389.
7. J. Xu, S. An, X. Song, Y. Cao, N. Wang, X. Qiu, Y. Zhang, J. Chen, X. Duan, J. Huang, W. Li and Y. Wang, *Advanced Materials*, 2021, **33**, 2105178.
8. G. Wen, X. Zhang, Y. Sui, K. Rao, J. Liu, S. Zhong and L. Wu, *Chemical Engineering Journal*, 2022, **430**, 133041.
9. X. Bai, X. Wang, T. Jia, L. Guo, D. Hao, Z. Zhang, L. Wu, X. Zhang, H. Yang, Y. Gong, J. Li and H. Li, *Applied Catalysis B: Environmental*, 2022, **310**, 121302.
10. S. B. Dhanalekshmi, R. Priya, K. Tamizh Selvi, K. Alamelu Mangai, G. K. Weldegebrieal, S. Garg and S. Sagadevan, *Inorganic Chemistry Communications*, 2021, **131**, 108768.
11. C. Tian, B. Li, X. Hu, J. Wu, P. Li, X. Xiang, X. Zu and S. Li, *ACS Applied Materials & Interfaces*, 2021, **13**, 6229-6240.
12. H. Li, S. Chen, X. Jia, B. Xu, H. Lin, H. Yang, L. Song and X. Wang, *Nature Communications*, 2017, **8**, 15377.
13. Z. Feng, P. Yang, G. Wen, H. Li, Y. Liu and X. Zhao, *Applied Surface Science*, 2020, **502**, 144129.
14. G. Nagaraju, C. N. Tharamani, G. T. Chandrappa and J. Livage, *Nanoscale Research Letters*, 2007, **2**, 461.
15. Y. Gao, C. Chen, X. Tan, H. Xu and K. Zhu, *Journal of Colloid and Interface Science*, 2016, **476**, 62-70.
16. E. Ghaleghafi and M. B. Rahmani, *Physica E: Low-dimensional Systems and Nanostructures*, 2022, **138**, 115128.
17. S. Krithika and J. Balavijayalakshmi, *Materials Today: Proceedings*, 2022, **50**, 17-25.
18. S. Zeng, F. Jia, B. Yang and S. Song, *Hydrometallurgy*, 2020, **195**, 105369.
19. M. Mousavi, A. Habibi-Yangjeh and M. Abitorabi, *Journal of Colloid and Interface Science*, 2016, **480**, 218-231.
20. R. G. Pearson, *Inorganic Chemistry*, 1988, **27**, 734-740.
21. S. Mohammadnejad, J. L. Provis and J. S. J. van Deventer, *Computational and Theoretical Chemistry*, 2017, **1101**, 113-121.
22. R. A. Bryce, J. M. Charnock, R. A. D. Pattrick and A. R. Lennie, *The Journal of Physical Chemistry A*, 2003, **107**, 2516-2523.
23. T. Lu and F. Chen, *Journal of computational chemistry*, 2012, **33**, 580-592.